JOURNAL OF MATERIALS SCIENCE 8 (1973) 1581–1589

Fracture behaviour of boron filaments

G. K. LAYDEN
United Aircraft Research Laboratories, East Hartford, Connecticut, USA

Various types of boron filaments were broken in tension in such a way that primary fracture surfaces, and fragments ejected when fracture occurred, were retained. Fracture surfaces observed in the scanning electron microscope could be placed into one of two broad categories. Type I surfaces exhibited primary fracture characteristics such as mirror, mist and hackle zones. Flaws which initiated failure could frequently be resolved. Type II surfaces appeared to be generated by subsequent fracture immediately following primary failure. The relationship between the fracture surfaces and the stress distributions occurring within the fibres as a result of manufacturing conditions is discussed.

1. Introduction

Boron filament is a brittle material. Its strength is controlled by structural imperfections or flaws. Earlier investigators [1-3] have discussed the fracture of boron filaments and have described various types of flaws including abnormal nodular growths, crystalline growths, bulk and core interface inclusions, notches in the tungsten substrate, and pre-existing crack tips. Wawner [1, 2] found that the majority of tensile failures originated at the surfaces of the filaments he tested but that in filaments chemically polished to remove surface flaws, fracture usually originated at the boron-core interface. Lasday and Talley [4] pointed out that various fibre manufacturing runs were characterized by different types of flaws so that results of etching are as variable as the flaw distributions of the filaments being etched. In the present study, the fracture behaviour of 4×10^{-3} and 5.6×10^{-3} in.* boron filaments of the type currently produced was examined. The fracture behaviour of boron filaments currently being manufactured is similar in some respects to that described earlier, but there also appear to be some fundamental differences that probably relate to different states of residual stress that result from different processing conditions.

2. Internal stresses in boron filaments

Vapour deposited boron filaments exhibit high residual stresses which strongly influence their mechanical properties [2, 5]. Internal stress measurements have shown the core of some filaments to be in residual compression of 150 to 200 $\times 10^3$ psi† [2]. A residual surface compression on the order of 70×10^3 psi, and a residual tension in the boron immediately adjacent to the core of about 120×10^3 psi have been calculated from the curvature of split filaments [2]. Recent direct measurements of internal stresses by Prewo and Douglas [6] based on changes in length of filament as the surface was progressively etched away show that residual compression in the first 0.1 mil of surface material can be as high as 900×10^3 psi.

During the deposition of boron on a tungsten substrate, the tungsten is progressively transformed into tungsten borides and the boron-core interface moves out from 0.5×10^{-3} in. diameter to about 0.65×10^{-3} in. This growth in volume of the core has been credited as the primary cause of the residual stresses. Other factors have also been suggested as contributing to the internal stresses, such as temperature fluctuations during deposition, thermal expansion difference between bulk and core, and the severe quench in the mercury seals [2]. It is probable that the very high state of residual compression in the surface of boron currently being manufactured results from the severe quench at the reactor exit seal. A further

* 1 in. = 2.540 cm.
† 1 psi = 6.895×10^3 Nm^{-2}.

mechanism for generating internal stresses has received little attention until quite recently. Talley [7] originally reported that boron rods deposited on tungsten filament elongated about 10% during deposition. Several years ago, Bourdeau [8] observed that boron deposited on carbon substrates fractured the carbon core into many short segments after a small amount of deposition and attributed this to axial growth of the boron to which the core could not respond. Recently, Diefendorf and Mehalso [9] studied the axial growth of boron deposited on carbon in more detail. They have shown that the elongation varies nearly linearly with the thickness of the boron deposit over most of the deposition period, and that the axial growth rate decreases with increasing deposition temperature. This growth can be accommodated only if either (1) volume dilation (decrease in density) occurs in previously deposited layers, or (2) a radial flow of amorphous material occurs during deposition in response to the growth stresses. Measurements of the density of the boron deposits of from 3×10^{-3} to 15×10^{-3} in. in diameter indicate no significant differences in density, thus indicating that boron must flow plastically during the deposition process. The driving force for the growth of boron has not been elucidated, but would appear to involve a very high surface tension of the amorphous boron imposing a shorter average bond length in the surface than subsequently occurs in the bulk.

It has been held that there is a radial crack in all boron filaments resulting from the internal stress situation [2, 10]. It will be shown later in this paper that the existence of a radial crack is by no means universal. However, the residual stress distribution in much currently produced filament results in a tendency toward splitting and has a marked influence on the transverse tensile properties. Kreider and Prewo [5] have discussed the transverse strength of boron filament in terms of residual stresses and radial flaws. It is interesting that they found the transverse strength of 5.6×10^{-3} in. boron to be substantially higher than that of 4×10^{-3} in. boron, and concluded that the radial flaw model probably does not control transverse filament fracture for the large diameter filaments. This picture is consistent with the observation of continual axial growth of boron. Since the core is not an infinite sink for boron but tends toward a limiting configuration, whereas the boron outside the core continues to grow, at some particular diameter one can expect a relaxation of the stresses at the core-boron interface which tends to initiate splits in the boron. Presumably, at greater filament diameters, a stress reversal would occur in the interface region with the core being placed in tension.

Given all the possible mechanisms for generating residual stresses in boron filament and the many possible interactions resulting from variations in process parameters, it is not surprising that different boron filaments show different fracture characteristics. Not enough is known at present about the relation of stress profiles to process conditions to optimize filament properties, but studies of fracture behaviour should prove helpful in sorting out these relationships.

3. Experimental procedure

4 in. samples were removed from suppliers spools at approximately 6 ft ($\simeq$ 1.83 m) intervals and placed sequentially into three groups. Samples from one group were removed at random and tested as described below, while the other groups were retained for future examination.

Boron fibres broken in tension recoil after fracture and generally break again closer to the grips so that the initial fracture surfaces are lost. Therefore, it is necessary to damp the recoil in order to retain the initial fracture surfaces for examination. The filaments were embedded in a layer of clear petroleum jelly held between two glass microscope slides supported on the filament mounting fixture. The petroleum jelly not only damped the recoil of the fibres, but also served to retain the tiny fragments which were ejected on fracture. The fixture was mounted in an Instron testing machine and samples loaded to fracture at a crosshead rate of 0.05 in. min^{-1}. (2.12×10^{-3} cm sec^{-1}). As soon as possible after fracture occurred, the crosshead motion was stopped and the fixture grips locked in position. The fixture was then transferred to the stage of a binocular microscope, where the degree of fragmentation could be assessed and photographs taken. The two opposing ends were then extracted, cleaned in trichloroethylene to remove the petroleum jelly, given a thin coating of palladium-gold alloy, and examined in the scanning electron microscope.

4. Results and discussion

The fracture of boron filaments is similar to the fracture of glass. The essential characteristics of

the fracture behaviour of glass have been summarized by Argon [11]. When glass rods are broken in tension, three regions are visible. The surface characteristics of each region depend upon the crack velocity in that region. The region in the vicinity of the initiation site (mirror zone) is smooth. As the crack accelerates, the surface roughens and takes on a matt appearance in the second region (mist zone) When maximum crack velocity is reached, distortions of the stress field cause portions of the crack front to deviate randomly above and below the intitial crack plane. The multiple advancing cracks join up in steep ridges resulting in characteristic markings (hackle zone). The tensile stress that caused failure in glass and some other brittle materials has been found to be inversely proportional to the square root of the radius of the mirror zone. This empirical relationship has been discussed by Johnson and Holloway [12] in terms of the energetics of crack propagation.

4.1. Features of boron fracture surfaces

All of the fracture surfaces examined could be placed into one of two very broad categories: (I) those which exhibited primary fracture markings over most of their areas and usually supplied information about the nature of the initiating flaw, or (II) those which displayed smooth secondary fracture surfaces which appear to propagate relatively slowly from the primary fracture surface after the initial failure.

4.1.1. Type I surface features

For type I fracture surfaces, in general, the point of initial fracture can be located by tracing back the hackle marks. In the case of 4×10^{-3} in. filaments, it has almost always been possible to trace these fracture paths back to the mirror zone and to the flaw that initiated failure. In the case of 5.6×10^{-3} in. boron, however, when fracture initiates in the core region, frequently a small secondary fracture will occur in the neighbourhood of the core and the initiation site will be lost. This tendency of the 5.6×10^{-3} in. boron to behave differently from the 4×10^{-3} in. filaments in the interface region probably relates to the quite different state of residual stress in this region for the two diameters alluded to earlier.

Figs. 1 and 2 show core initiated type I fracture surfaces exhibited on commercial 4×10^{-3} in. boron filament from two different suppliers. Examination of the fractured ends in the binocular microscope while they were still embedded in the petroleum jelly showed that a small mass of tiny wedge-like fragments was ejected at fracture, leaving the shallow conical surfaces on the broken filament ends. In both instances surface markings can be traced back to the intitial fracture sites within the cores. These two examples differ in four obvious respects; namely (1) the radial position within the core where fracture initiated, (2) the angle of the conical surface with respect to the filament axis, (3) the degree or scale of the hackle markings, and (4) the degree of turning of the advancing crack fronts as they approach the surface (skin effect). In all these respects the examples shown are typical of the appearance of core initiated

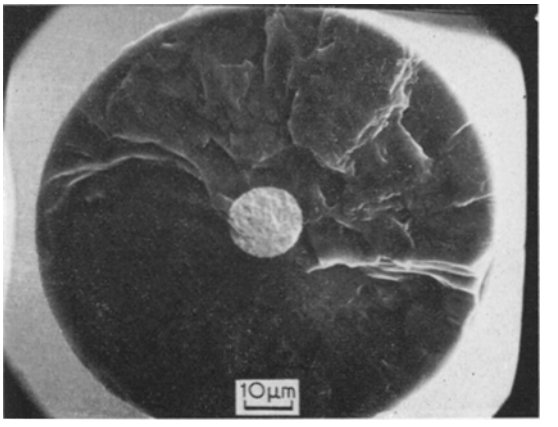

Figure 1 Core initiated type I fracture surface of 4×10^{-3} in. boron filament from supplier A. Stress at fracture of this specimen was 570×10^3 psi.

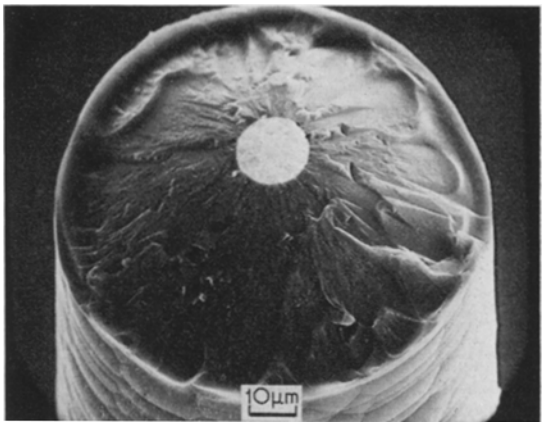

Figure 2 Core initiated type I fracture surface of 4×10^{-3} in. boron filament from supplier B. Stress at fracture of this specimen was 620×10^3 psi.

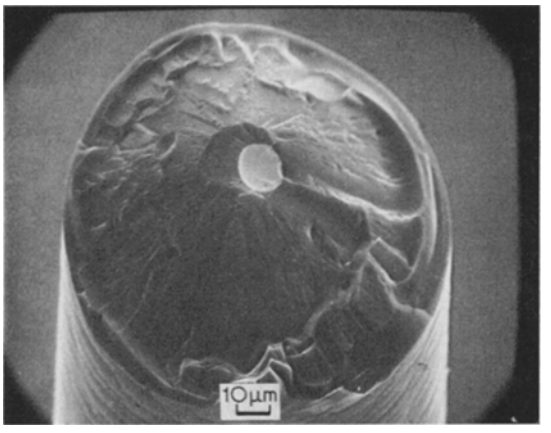

Figure 3 Type I fracture surface initiated in core or interface region of 5.6×10^{-3} in. boron filament. Stress at fracture 575×10^3 psi.

fractures exhibited by 4×10^{-3} in. filaments from the respective suppliers.

Fig. 3 shows a fracture surface that is characteristic of type I surfaces initiated in the core region of 5.6×10^{-3} in. boron. The surface exhibits many features in common with fractures of 4×10^{-3} in. boron, except that a chip or crater has been ejected from the core area taking with it the initial fracture site. These crater surfaces are smooth, indicating slow crack propagation, but the absence of a mist or transition zone between these surfaces and the surrounding hackle zones precludes the possibility that these are the initial fracture mirror zones. This observation has been substantiated by finding several instances where one fracture surface contained all three zones and the initial flaw could be located, whereas the opposing fracture surface was similar in all respects except for the presence of the chip or crater. In still other instances, part of the initial mist zone was still in evidence on the lip of the crater. It is thus apparent that the core-chipping occurred after the initiation of the primary fracture. It seems likely that stress points on the newly created free surfaces initiate secondary fractures that propagate in response to the residual stresses built into the filaments. This type of mechanism will be discussed more fully in the section on type II fracture surfaces.

Many features of the type I surfaces (cone angle, scale of the hackle, "skin effect") depend upon the amount of forking or branching of the initial crack which, in turn, probably depends upon the amount of strain energy released in each increment of fracture. While, in general, it would appear that steeper cone angles are associated with higher stresses at fracture, the magnitude of the residual stresses and their distribution across the filament profile must have a strong influence on the incremental release of strain energy.

Fig. 4 is a conceptual sketch of the fracture patterns within two filaments which exhibit different degrees of crack branching an instant before they part and, below, the resulting fracture surface characteristics. The branching of the cracks drawn here may be compared to the photographs of branching cracks in plate glass resulting from progressively more energetic blows on a chisel taken by Schardin [13] and reproduced by Argon [11]. In the case of little branching sketched in Fig. 4, all crack fronts reach the surface nearly normal to the filament axis at nearly the same time. Consequently, the cracks that will become the surfaces of the two severed halves travel with near maximum velocity right out to the filament surface and little "skin effect" is observed. This is the type fracture surface shown in Fig. 1. However, when there is considerable branching of the advancing crack fronts, progressive cracks travel at decreasing angles to the filament axis. Cracks travelling at lower angles are still some distance from the filament surface when those travelling normal to the axis break through the surface. When this occurs, the strain energy associated with the externally applied stress has been dissipated and only internal energy associated with the residual stresses in the filament can supply energy to the still advancing low-angle cracks. These cracks then slow down abruptly and present the relatively smooth appearance near the surface seen in Figs. 2 and 3. The sudden turning of these rapidly decelerated cracks is probably the result of a tendency of the cracks to re-align themselves normal to the principal stresses in the rapidly changing residual stress field.

4.1.2. Flaws observed on type I fracture surfaces

Four types of flaws were encountered in this study. One of these flaws causes surface initiated fracture, although the origin of the flaw has been traced back to the interior of the filament, usually the tungsten substrate surface. The other three cause centrally initiated failures. Two of the types of flaws, namely, the abnormal nodular growth and the proximate flaw, were observed

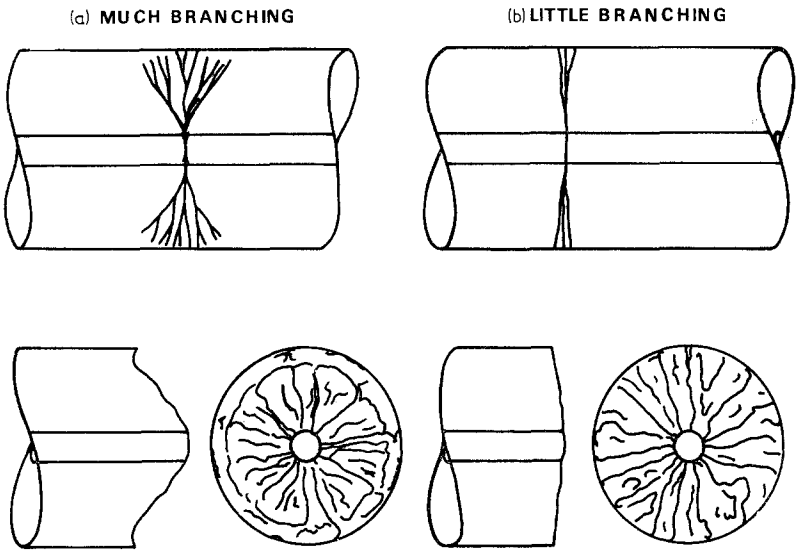

Figure 4 Conceptual relation of type I fracture surface characteristics with the degree of initial crack branching.

only on some spools of 5.6×10^{-3} in. boron from one supplier and appear to be related to contaminants on the substrate.

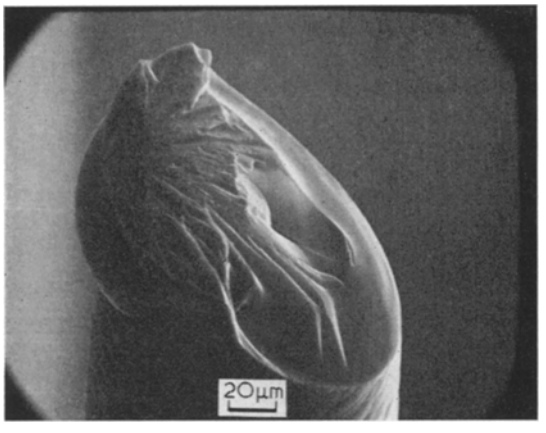

Figure 5 Fracture initiated at an abnormal nodular growth at the surface of 5.6×10^{-3} in. boron. Stress at fracture was 215×10^3 psi.

4.1.2.1. Abnormal nodular growth

An example of this flaw is shown in Fig. 5. Flaws of this type caused failure at around 200×10^3 psi. This type of flaw has been discussed by Line and Henderson [3] who related it to accentuated growth around a contaminant particle on the substrate surface or some other inclusion within the bulk of the boron.

4.1.2.2. Proximate flaws

This is a class of flaws of variable severity that was encountered on fractured samples from several spools of 5.6×10^{-3} in. boron. These flaws were located in the boron in close proximity to the core and consisted of more or less irregularly shaped voids or tears similar to that shown in Fig. 6. They controlled strength in the range from 200×10^{-3} to over 500×10^3 psi. Electron microprobe analysis of one such example disclosed a local concentration of iron associated with the void.

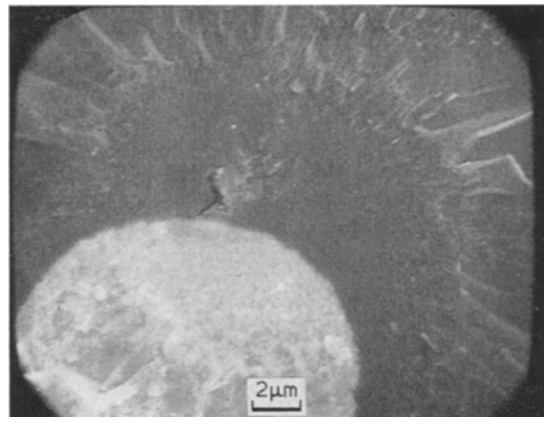

Figure 6 Fracture initiated at an irregular void just outside of the boron-core interface. Stress at fracture was 244×10^3 psi.

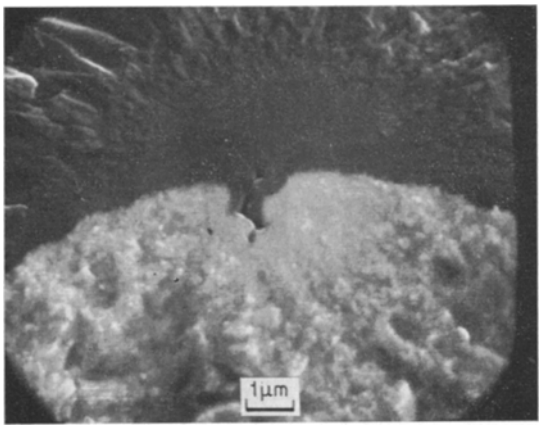

Figure 7 Fracture initiated at an occluded void at the boron-core interface resulting from a notch in the tungsten substrate. Stress at fracture was 370 × 10^3 psi.

4.1.2.3. Interface notch

An example of a characteristic interface flaw which controlled strength in the range of from about 300 × 10^3 to 550 × 10^3 psi is shown in Fig. 7. This type of flaw results from a deep groove or notch in the original tungsten substrate. Longer diffusion paths for gaseous reactants and products result in slower deposition of boron at the bottom of the notch than at the surface which frequently leads to the occlusion of a void within the notch. Convolutions on the internal surface constitute the stress concentration points that initiate failure.

4.1.2.4. Core interior

In the absence of flaws due to substrate defects or contamination, fracture of the boron filaments originated within the core. Fig 8 shows the fracture initiation site deep within the core of a 4 × 10^{-3} in. filament. Fractures of this type occur at the highest stress levels encountered and exhibit the lowest variability in strength. Core initiated fracture of samples from a given spool can exhibit a coefficient of variation below 2%. The radial location of the fracture initiation site within the core is reasonably constant for filament made under similar conditions, and appears to be a characteristic feature, along with cone angle, hackle, and skin effect, of filament of a given diameter from different suppliers. The significance of this characteristic fracture-site radius in terms of core development or substructure has yet to be determined.

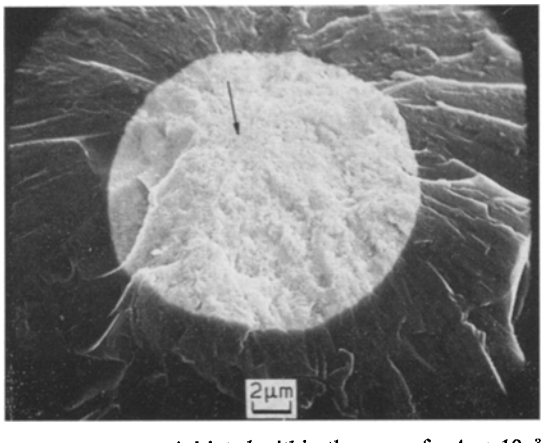

Figure 8 Fracture initiated within the core of a 4 × 10^{-3} in. boron filament. Stress at fracture was 600 × 10^3 psi. Arrow points to initial failure site.

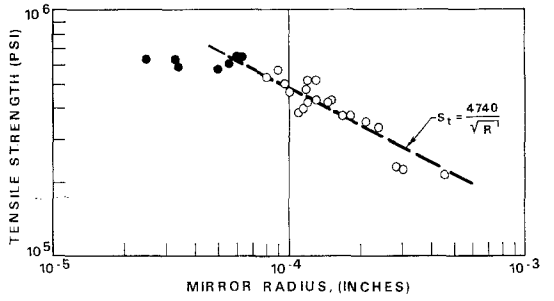

Figure 9 Relation between mirror radius and tensile strength of boron filaments. Fractures initiated within the cores are shown by solid points, fractures initiated at flaws in the boron are shown by open circles.

4.1.3. Relationship between strength and mirror radius

The radii of the mirror zones have been measured on scanning micrographs of type I fracture surfaces. The curve of calculated stress at failure versus mirror radius is shown in Fig. 9. The (unknown) additive effect of the initial residual stress in the mirror region has not been taken into account in presenting these data and the stresses are calculated from the external load only. There is considerable scatter in the data owing, in part, to the difficulty of deciding on the boundary of the mirror zone in low magnification micrographs, and also no doubt to the variable effect of the residual stress state. However, it would appear from Fig. 9 that the stress at failure follows the $R^{-1/2}$ empirical relationship found for other brittle materials.

4.1.4. Type II surface features

Fig. 10 shows a characteristic fracture surface of

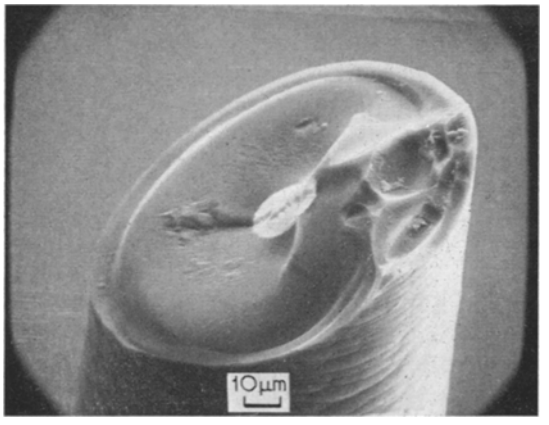

Figure 10 Type II fracture surface of 4×10^{-3} in. boron filament. Stress at fracture of this specimen was 560×10^3 psi.

a type that has been found on both 4×10^{-3} and 5.6×10^{-3} in. boron. Under the binocular microscope, it was observed that several large fragments had separated from the filament ends in cases where this type of surface was exhibited. The surfaces exhibited on the two remaining filament ends are thus located some distance back (typically about one filament diameter) from the point at which failure initiated. These surfaces are relatively smooth indicating that the cracks propagated quite slowly despite the fact that strengths of the order of 600×10^3 psi were recorded for such fractures. Some hackle marks are evident on the principal surfaces, particularly in the case of the 5.6×10^{-3} in. filament which indicate the direction which these cracks travel. Surfaces of this type usually exhibit three principal markings or rays which appear to originate (or terminate) in the core. These rays usually make angles of nearly 120° when measured near the core. Two of these rays describe a pattern that might best be described as a pair of "gull wings". These "gull wings" appear to define two converging helical surfaces that turn down into a cusp which is the third of the principal markings. Beyond the end of each "gull wing" is a region where the direction of propagation of the principal crack appears to be reversed as though pivoted about the end of the wing. These two principal crack surfaces then sweep together and join in a rough region where the severed fragment finally broke away.

One fracture of 4×10^{-3} in. boron filament produced a pair of fracture surfaces that is particularly revealing as to the genesis of these type II or secondary surfaces. One-half of the filament retained the hackled primary fracture surface over its entire area. The opposing end retained the primary fracture surface over part of its area, but displayed a single smooth helical surface extending down from the initial surface and terminating at a vertical step or radial crack. The helical surface appeared to have the characteristics of the principal surfaces seen in Fig. 10. It seems likely that the type II fractures propagate from the primary fracture surfaces after the initial event has occurred, and that the stresses that drive these relatively low velocity cracks are the residual stresses in the filaments.

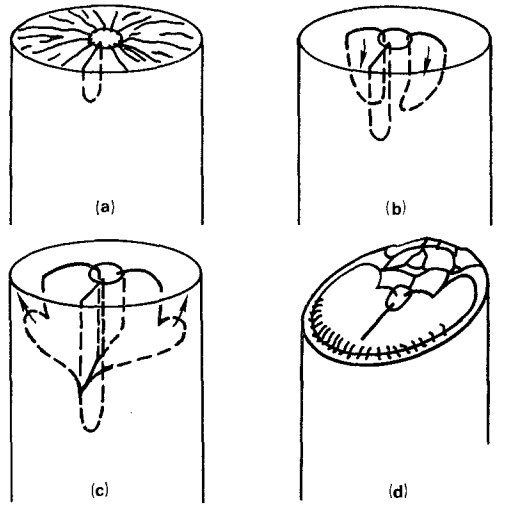

Figure 11 Conceptual model for the generation of type II surfaces. See text for details.

A plausible model for the creation of type II fracture surfaces is sketched in Fig. 11. When a normal tensile failure (type I) occurs a free surface is generated which is covered with steep radial steps (hackles) which can serve as stress risers or flaws for the initiation of radial cracks in the region of the filament which is in a state of residual tension (Fig. 11a). When a radial crack appears and begins to propagate, this fixes the most probable position for other radial cracks to appear at 120° separations since this gives an efficient scheme for stress relief (Fig. 11b). These subsequent cracks appear to be "sucked into" the initial crack (for reasons that are not immediately obvious but again probably involve the dynamics of the rapidly changing residual stress field) and to pivot around behind the initial

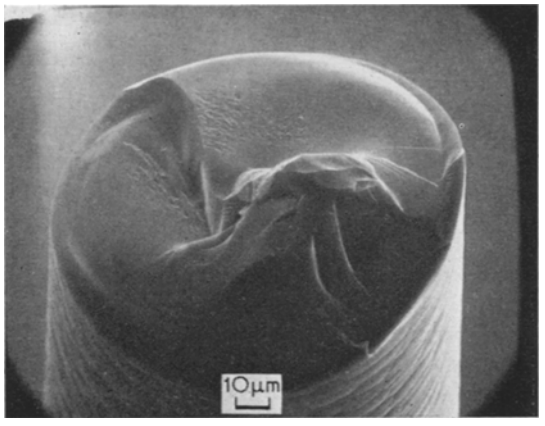

Figure 12 Non-symmetrical type II surface resulting from uneven distribution of secondary cracks.

outer crack termination in the compressive region (Fig. 11c). Final separation in the rough area behind the gull wings leaves the fracture surface shown in Fig. 11d.

In most cases where type II surfaces have been observed, the three principal markings are at about 120° separation, and this leads to the bilaterally symmetrical surfaces shown in Fig. 10. Occasionally, however, cracks are not equally spaced and this leads to some interesting non-symmetrical surfaces. One such surface is shown in Fig. 12.

Both type I and type II surfaces have been found on filaments which fractured at stress levels ranging from 200 × 10^3 to well over 600 × 10^3 psi. While some spools of boron filament show a preponderance of one or the other type fracture surface, both types have been exhibited on samples from the same spool. Type I fracture samples from the same spools that exhibited type II surfaces generally did not exhibit radial splits, thus it seems doubtful that radial splits existed in the filaments that exhibited type II fractures prior to testing. On the other hand, 4 × 10^{-3} in. boron filament made under experimental conditions of very high deposition rate and high rate of travel through the reactor (over 1200 ft h^{-1}) resulting in extremely severe quench at the exit mercury seal did exhibit radial cracks on type I surfaces. In cases where this has been observed, one or the other end of the radial split appears to serve as the initiation site for tensile failure.

5. Summary

Boron filament fracture surfaces can be divided into two major categories. Type I surfaces generally exhibit the mirror, mist and hackle zones familiar from studies of glass fracture. Flaws which initiated failure can frequently be resolved in the scanning electron microscope. Type II surfaces are relatively smooth and appear to originate at steps on newly created type I surfaces and are propagated by the internal residual stresses in the filaments. Core initiated failures predominate in current commercial boron filaments in contrast to reports of earlier studies where surface initiated failures predominated. The absence of surface initiated failures (excepting those initiated at abnormal nodular growths) in current boron filaments is probably related to a very high residual surface compressive stress.

Acknowledgements

The author is indebted to V. M. Patarini and L. Jackman for the scanning microscopy, to A. V. Manzione for electron probe measurement studies, and to K. M. Prewo for many stimulating discussions and his critical review of the manuscript.

References

1. R. E. WAWNER, in "Boron", Vol. II, edited by G. K. Gaule (Plenum Press, New York 1965) pp 283-300.
2. *Idem*, in "Modern Composite Materials", edited by L. J. Broutman and R. H. Krock (Addison Wesley, Reading, Mass, 1967) pp. 244-269.
3. L. E. LINE, JUN. and U. V. HENDERSON, in "Handbook of Fiberglass and Advanced Plastic Composites", edited by G. Lubin (Van Nostrand Reinhold, New York, 1969) pp. 201-236.
4. A. H. LASDAY and C. P. TALLEY, in "Advanced Fibrous Reinforced Composites", (Society of Aerospace Material and Processing Engineers, Vol. 10 Azusa, California, 1966) pp. D1-D12.
5. K. G. KREIDER and K. M. PREWO, "Composite Materials: Testing and Design" (Scond Conference) ASTM STP 497 (American Society for Testing and Materials, Philadelphia, 1972) p. 539.
6. K. M. PREWO and F. DOUGLAS, personal communication, to be published.
7. C. P. TALLEY, *J. Appl. Phys.* **30** (1959) 1114.
8. R. G. BOURDEAU, in United Aircraft Research Laboratories Report G110550-2 (1968).
9. R. J. DIEFENDORF and R. M. MEHALSO, in Technical Report AFML-TR-70-287 (1971).
10. R. P. I. ADLER and M. L. HAMMOND, *Appl. Phys. Letters* **14** (1969) 354.
11. A. S. ARGON, in "Mechanical Behaviour of Materials", edited by F. A. McClintock and A. S. Argon (Addison Wesley, Reading, Mass, 1966) pp. 500-504.

12. J. W. JOHNSON and D. G. HOLLOWAY, *Phil. Mag.* **14** (1966) 731.
13. H. SCHARDIN, in "Fracture", (edited by B. L. Averbach, D. K. Felbeck, G. T. Hahn and D. A. Thomas M.I.T. Press, Cambridge, Mass, and Wiley, New York, 1959) p 394.

Received 26 March and accepted 5 June 1973.